Soil-Bioengineering to Stabilize Gravel Roadside Slopes in Steep Hyrcanian Forests of Northern Iran

Soghra Keybondori [1], Ehsan Abdi [1*], Azade Deljouei [2], Alessio Cislaghi [3,4], Zahed Shakeri [5], Vahid Etemad [1]

1. Department of Forestry and Forest Economics, Faculty of Natural Resources, University of Tehran, Karaj, Iran

2. School of Forest, Fisheries, and Geomatics Sciences, University of Florida, Gainesville, FL, USA

3. Department of Agricultural and Environmental Sciences, University of Milan, Milan, Italy

4. Centre of Applied Studies for the Sustainable Management and Protection of Mountain Areas, University of Milan, Edolo, Brescia, Italy

5. Department of Forestry and Conservation, Daniels Faculty, University of Toronto, 33 Willcocks Street, Toronto, Ontario, M5S 3B3

*** Corresponding author: abdie@ut.ac.ir (E. Abdi)**

ORCID of the authors:

- Ehsan Abdi: 0000-0002-3382-7683
- Azade Deljouei: 0000-0003-3453-8530
- Alessio Cislaghi: 0000-0002-4618-818X
- Zahed Shakeri: 0000-0002-1068-3218

Abstract

Soil-bioengineering techniques for stabilizing road cut and fill slopes based on indicator herbaceous and woody species in the Hyrcanian Forests of Northern Iran effectively reduce shallow landslide occurrences and improve overall slope stability. We assessed the role of roots in stabilizing shallow soil layers by measuring the root biomechanical properties and root distribution of 13 indicator species, from cut and fill slopes. Our study identified *Athyrium filix-femina* and *Pteris cretica* as the most effective species for slope stabilization on cut slopes, providing root reinforcement values of 4538 Pa and 4513 Pa, respectively, and reducing slope instability by up to 18%. On fill slopes, *Sambucus ebulus* and *Phyllitis scolopendrium* showed significant root reinforcement potential, reducing slope instability by up to 17% and 18%, respectively. The root systems of these species were primarily concentrated in the upper 0.1 m to 0.2 m of soil, providing simultaneously soil reinforcement and erosion control. The study indicated that in the Hyrcanian Forest, where favorable climate conditions prevail, native pioneer species were particularly effective for slope stabilization, especially in areas without natural vegetation. Over the time, this approach can restore disturbed areas, enhance biodiversity, and improve forest health. As a sustainable alternative to traditional methods, it offers forest managers a practical solution for reducing landslide risks and fostering ecosystem resilience. While these results highlighted the potential of herbaceous vegetation in mitigating slope failures, soil type and local climate may influence their effectiveness. Consequently, site-specific applications and further research needed to optimize vegetation selection for long-term slope stability. This study provided a framework for integrating native plants into soil-bioengineering techniques for forest road management, promoting environmental sustainability and ecosystem resilience.

Keywords: Herbaceous vegetation, Hyrcanian temperate forests, Root maximum tensile force, Root reinforcement, Shallow landslides, Species importance value, Slope stability

1. Introduction

The appropriate construction and maintenance of forest roads are essential for ensuring safe access, sustainable forestry, infrastructure development and economic growth. However, poorly planned road construction can lead to significant landscape disturbances, including the loss of vegetation cover, disruption of natural drainage patterns, and occasional flooding. These changes exacerbate erosion, and in the ultimate trigger, landslides, especially in steep mountainous regions (Liniger and Weingartner, 2000, Mao et al., 2012; Murgia et al. 2022). Prior to the excavation of forest roads in Iran, all trees within the designated right of way are removed, which exposes gravel roadbeds to the drying effects of sunlight and wind by removing the canopy. Natural revegetation is expected to occur on cut and fill slopes due to favorable climatic and environmental conditions over the time. However, in certain restricted regions, the timely introduction of pioneering grasses and various herbaceous plants is undertaken to facilitate the natural restoration process. The road is then periodically maintained to prevent mature tree and shrub from encroaching onto the roadbed, shoulders, and drainage ditches. These herbaceous plants and the woody seedlings that occur naturally play a crucial role in reducing erosion and enhancing slope stability and biodiversity in the area (De Baets et al., 2008; Löbmann et al., 2020).

The construction of steeper cut and fill slopes initially denuded by vegetation, requires careful timing to prevent landslides during the wet seasons when fine-grained soils on unstable slopes become saturated. Scheduling the most appropriate period when adequate soil moisture is available to facilitate rapid revegetation through planting or natural recolonization by native plants is a key aspect in the construction, moreover, unpaved forest roads are commonly prone to damage during spring thaw and during poorly planned maintenance involving vegetation removal (Gray and Sotir, 1996). Employing native herbaceous plants to stabilize steep slopes offers a sustainable, cost-effective, and efficient

first step due to the adaptability and ability to grow in diverse climates and on different soil types (Cazzuffi et. al., 2006, Rey et al., 2019).

Green renewable soil bioengineering techniques that use grasses, shrubs, and trees for slope stabilization has been practiced in Europe since at least the early twentieth century (Schiechtl, 1980; Giupponi et al., 2019; Bischetti et al., 2021). Pioneer herbaceous species typically regrow after disturbances faster than trees, covering slopes and promoting the succession of shrubs and trees. Once forests are reestablished, understory herbaceous cover continues to play a crucial role in minimizing soil loss. Seasonal root dieback also reduces runoff and favor retaining more soil moisture (Vergani and Graf, 2015). Herbaceous cover significantly contributes to minimize soil saturation, which often causes instability on steep slopes, while plant transpiration from aboveground tissues reduces the risk of landslides (Mulyono et al., 2018; Bordoloi and Ng, 2020).

Moreover, plant roots increase the shear resistance primarily by anchoring and binding soils, a process that is influenced by both soil and plant characteristics. In fact, soil factors such as moisture content, nutrient availability, depth, mechanical properties, hydrological properties, slope gradient, and temperature directly affect root growth and the rooted-soil cohesion (Lann et al., 2024). These factors determine how effectively roots can stabilize slopes by maintaining biomechanical adhesion with the soil. Nevertheless, root spatial distribution and root biomechanical properties are the key parameters for stabilizing shallower soil layers (Vergani et al., 2014). Local growth conditions such as stand origin, structure, and the spatial arrangement of species further influence plant characteristics such as species composition, root morphology, root mechanical strength, and root density (Stokes et al., 2008; Fan, 2012; Cislaghi et al., 2021; Mao et al., 2012, 2018, 2023).

Several models have been developed based on root distribution and root biomechanical properties to estimate root reinforcement and assess landslide susceptibility on vegetated

slopes. The models developed by Wu (1976; Wu et al., 1979) and later by Waldron (1977) conceptualize roots as fibers perpendicular to the shear plane of slope failure but differ in some important aspects. Wu's model emphasizes load-sharing among tension-dominated roots and introduces a correction factor for root failure at different times, conversely, the Waldron's approach incorporates composite root strength into the Mohr-Coulomb equation, assuming simultaneous failure of all roots, which oversimplifies the dynamics of root failure (Waldron, 1977). Both models were criticized for overestimating slope stability (Schwarz et al., 2013). More sophisticated models, such as fiber bundle models (FBM) by Pollen and Simon (2005), conceptualize roots as fibers resisting tensile forces that progressively redistribute as fibers break. The Root Bundle Model with Weibull survival distribution (RBM-Weibull) developed by Schwarz et al. (2013) further refines this approach by accounting for root spatial distribution and maximum tensile force. This model correlates root length, root tensile strength, and the average modulus of elasticity empirically with root diameter using calibrated power functions, making it a more robust tool for assessing slope reinforcement (Schwarz et al., 2015; Masi et al., 2021; Karimi et al., 2022).

All these models were applied for assessing the contribution of vegetation; however fewer explored the role of herbaceous and early successional species in forest understories where mature trees are absent (Dumlao et al., 2015; Gilardelli et al., 2017; Mao et al., 2023; Kettenhuber et al., 2023). Löbmann et al. (2020) concluded that solely taking vegetation type into account is inadequate for classifying slope stability achieved through soil-bioengineering techniques. Instead, they underscored the importance of species-specific attributes, ecological factors within vegetation communities, and growth conditions. Therefore, understanding species-specific attributes, such as root length and plant height, is crucial for evaluating and optimizing slope stability in bioengineering applications (Pohl et al., 2011). Depending on

121 local requirements, either woody or herbaceous vegetation may provide a higher degree of
122 slope stabilization, whereas in some cases, their effectiveness may be comparable.

123 On this background, this study aims to investigate the effect of vegetation on slope stability
124 by examining the influence of both herbaceous and woody species in the temperate forests
125 especially along forest roads. According to the Food and Agriculture Organization of the
126 United Nations, numerous regions across Asia are susceptible to landslides due to steep
127 terrain, vulnerable soils, heavy rainfall, and seismic activity (Sassa et al., 2017). The Alborz
128 Mountains, located in northern Iran, are particularly susceptible to landslides (Pirasteh and
129 Li, 2017), especially following anthropogenic activities such as infrastructure development.
130 In the Hyrcanian temperate forests, located along the northern slopes of the Alborz
131 Mountains, landslides frequently occur in disturbed soils near roads, riverbanks, and other
132 areas where vegetation cover has been removed (Moghaddas and Gafoori, 2007). Identifying
133 the specific traits of herbaceous and woody vegetation roots and canopies is essential for
134 recognizing pioneer species that can rapidly revegetate disturbed areas. These species can
135 stabilize the soil and mitigate the risk of slope failure and the excessive erosion until more
136 long-term, successional plants like shrubs and trees establish themselves. This approach helps
137 maintain slope stability and prevent further environmental degradation in erosion-prone
138 areas.

139 In Iran, before excavation for construction of forest roads in steep terrain, all obstructing trees
140 within the designated right of way, including both cut and fill slopes, must be marked and
141 removed, typically by cutting the trees and salvaging the useful wood. The timing of tree
142 removal should avoid critical wet periods when the bare slopes are the most unstable and
143 should allow the planting and establishment of herbaceous and other pioneer species to
144 swiftly minimize erosion and slope instability while accelerating succession to a plant
145 community that maximizes slope stability and sustainable forest resources.

This study was conducted on the Hyrcanian temperate forests of northern Iran and pursued four main objectives: (1) identify the key species that ultimately revegetate denuded steep roadsides following forest road construction; (2) select indicator species and measure the bio-mechanical characteristics of their roots; (3) estimate the root reinforcement provided by the indicator species using the Root Bundle Model with a Weibull survival distribution, and (4) holistically evaluate the contribution of trees, shrubs, and herbaceous plants in enhancing slope stability.

2. Materials and Methods

2.1. Study Site

This study was conducted in Kheyrud Experimental and Educational Forest, an 8000 ha site directly managed by the University of Tehran. This area is considered representative of key features typical of the Hyrcanian temperate forest ecoregion (Figure 1). The Hyrcanian mixed forests as designated by the Worldwide Fund, primarily lie along the southern coast of the Caspian Sea. This unique ecoregion spans from southeastern Azerbaijan through northern Iran, covering the northern slopes of the Alborz Mountains. The range extends approximately 850 km, from the Talish Mountains in Azerbaijan to the eastern extent of the Alborz Mountains in northern Iran. These forests are characterized by rich biodiversity and a unique mix of temperate broadleaf and mixed forest species that have persisted since the Tertiary period (Eghrari et al., 2023). While the flora includes some endemic species, many plant species belong to the Euro-Siberian flora kingdom, commonly found in temperate forests across Europe (see Flora Iranica (Rechinger, 1963), Flora of Iran (Assadi et al., 1989), and Flora of Turkey (Davis, 1984)).

The climate in the Hyrcanian forests is humid, with relatively limited temperature fluctuations. From 1977 to 2016, the mean annual precipitation was 1297 mm, and the mean

annual temperature averaged 16.5 °C in the study area (Dezhban et al., 2019). Kheyrud Experimental and Educational Forest is primarily underlain by calcareous bedrock deposited during the Jurassic Period, producing brown clays or calcic-brown clays (caliche) with both low and high liquid limits (CL or lean clay and CH or fat clay, respectively, based on the Unified Soil Classification System).

Namkhane district, the second of the seven districts of Kheyrud Experimental and Educational Forest, was selected as the study site (Figure 1). The elevation range in the district is 350 m to 1350 m above mean sea level. Soil was characterized as clays with high plasticity (CH), and geotechnical analyses provided the following mean values (±SD) for Atterberg limits: soil liquid limit (Casagrande cup method) was 88.5% (±7.4%), soil plastic limit (rolling and thread method) was 38.3% (±4.9%), and soil plasticity index was 50.2% (±4.6%). The range of effective soil cohesion (2 to 13.5 kPa) and internal friction angle (26° to 35°) used in the probabilistic shallow landslide model was derived from (Deljouei et al., 2023). The road network consists of 15.8 km (i.e., road density of 20 m ha^{-1}) of main forest roads (class II) that delineates the boundaries of compartments, along with some secondary roads (class III) that extend into these compartments. Main forest roads were selected for the study because of their greater length and broader coverage. The nominal roadbed width of main roads is 6 m, but the range varies from 5 to 9 m. Thus, only two-axle, 6-wheel trucks are used to transport wood in the Kheyrud Forest. The Namkhane road network was constructed in 1990 by bulldozers within 12 m to 15 m wide rights-of-ways centered on the roadbed axis and cleared of all trees and shrubs. Roads were formed by cutting a bench into landscape slopes averaging 17 degrees with a drain ditch between the toe of the cut slope and the roadbed. The substantial side cast fills and wasting, which formed the fill slope resulted in deep displacements of soil that generally do not benefit the remaining vegetation and can even damage trees and shrubs beyond the cleared right-of-way. A parallel downgradient ditch

was not cut into the fill slope. According to the Kheyrud Forest road maintenance guidelines, some tree seedling and shrubs on both roadsides are regularly cut to prevent sight distance obstruction.

This study selected a total of 8.7 km of the all-season main roads to identify and collect roadside vegetation as shown in Figure 1 (see Supplementary Materials Table S1). The major plant associations surrounding the main gravel roads in Namkhane, based on the Braun-Blanquet approach (Braun-Blanquet, 1913), include *Fagetum orientalis*, *Querceto-Carpinetum betulii*, and *Carpino-Fagetum orientalis*. The dominant tree species within these communities in the Hyrcanian Forest are *Fagus orientalis* Lipsky, *Carpinus betulus* L., *Parrotia persica* (DC.) C. A. Mey, *Acer cappadocicum* Gled., *Acer velutinum* Boiss., *Alnus subcordata* C.A. Mey, *Ulmus glabra* Huds., and *Quercus castaneifolia* C.A. Mey (Assadoallahi, 2001).

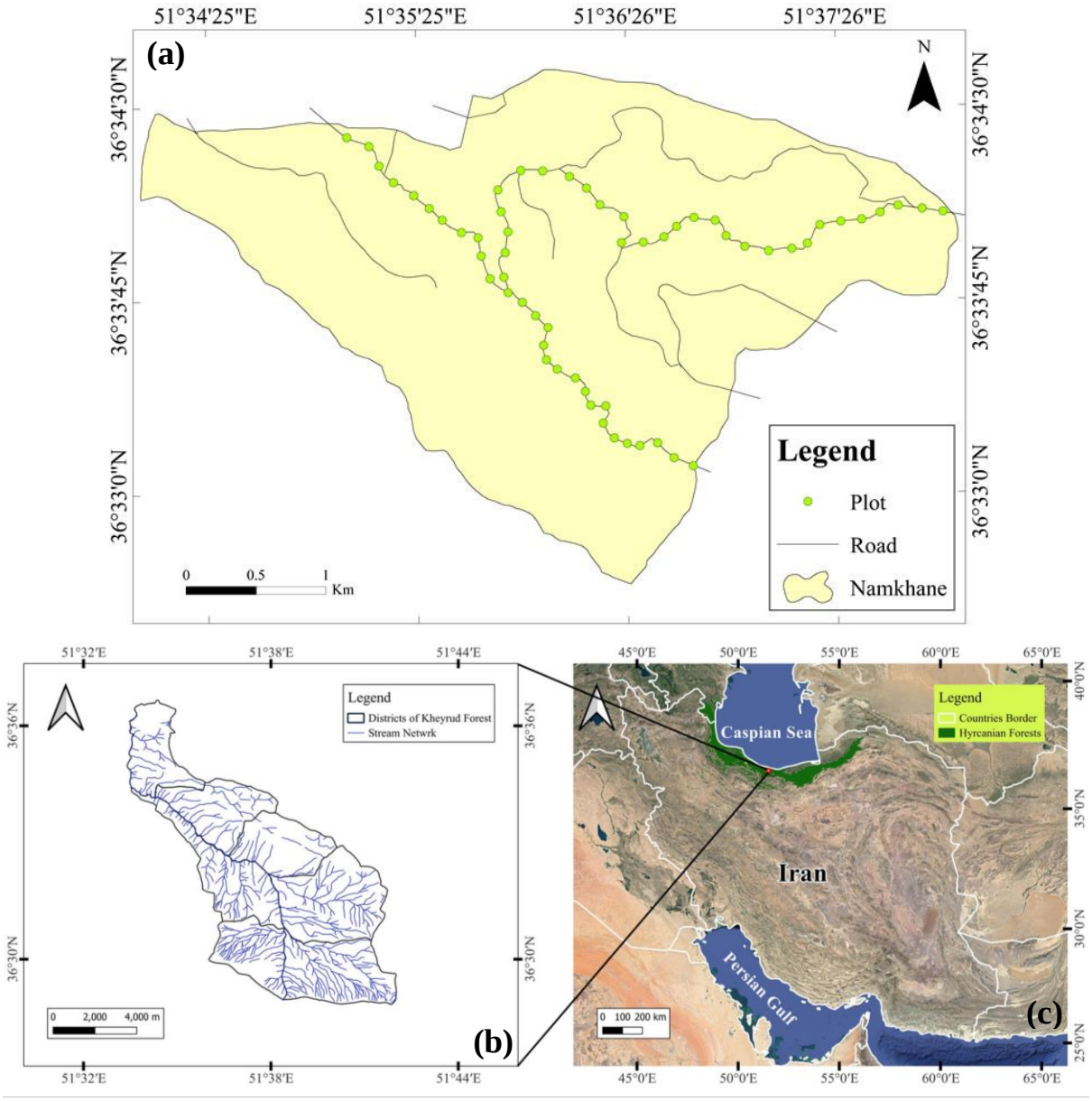

Figure 1. (a) Location of the 116 vegetation inventory plots on cut or on fill slopes along the main forest roads in the Namkhane District, (b) the seven districts of the Kheyrud Experimental and Educational Forest, and (c) the location of the Kheyrud Experimental and Educational Forest as a part of the Caspian Hyrcanian mixed forests ecoregion in the central Alborz Mountains of northern Iran.

2.2. Sampling Strategy

We conducted a systematic inventory of vegetation to select indicators species and then collected five root systems for each of the identified indicator species from July 10 to 24,

2020. Figure 1 shows the 58 locations of each pair of plots on both sides (cut and fill slope) of the main roads (see Figure S2 for more details). In the further phase, the vegetation inventory and collection of root systems from indicator species were conducted during relatively dry conditions when heavy rainfall was absent. However, the clay soil was moist enough so that root desiccation and dieback were not visually observed. Siadati et al. (2010) note that July is the peak of phenological development for most plants in the middle parts of the Hyrcanian Forest (e.g. Kheyrud Forest), especially for longer lasting species with substantial aboveground and belowground biomass necessary to stabilize steep slopes. Early-season species, such as short-lived therophytes may not have been inventoried, as such transient vegetation is unlikely to affect slope stability. The well-drained, cracked calcium carbonate bedrock of the Namkhane district has fissures and dissolution channels that limit the formation of perched water tables and thereby limit soil saturation, which can cause landslides. Consequently, percolated water freely drains to the Kheyrud River (Majnounian and Etter, 1992).

This study identified the vegetation species and their distribution on 116 plots, each measuring 20 m^2 (2 m width × 10 m length). Optimal plot area was determined using nested subplots and species-area relationships (van der Maarel, 2005; see the Supplementary Material Figure S1). Each plot, situated on either cut or fill slopes, had its lower boundary set 1 m away from the outer edge of the road (1 m beyond the ditch on cut slopes and 1 m beyond the fill slope shoulder). These plots were distributed across 58 locations, spaced at 150-m intervals along the centerline of the main roadbeds, starting from the western boundary of the Namkhane District (more details in Figure S2 in Supplementary Material). The mean ± standard deviation of slope gradient for plots on the cut slope was about 40.5 ± 19.4 degree and for fill slope was 33.8 ± 19.3 degree. The percentage of ground covered by tree canopy through visual assessment, a quick method that requires no specialized

241 equipment proposed by Jennings et al. (1999) and widely used by forest managers. To
242 determine canopy cover percentage, five observations were taken—one at the center and one
243 at each corner of the plot. The average percentage of ground covered by tree crowns from
244 these observations was recorded as the crown canopy percentage for the plot. The average
245 canopy cover over the 116 plots was 40 percent, classifying it as relatively open; thus, most
246 of the 116 plots were unshaded. Consequently, no succession of mature trees and shrubs
247 occurs on most of the cut and fill slopes due to road operations disturbance, especially within
248 1 m to 5 m from the edge of the roadbed. Roadside maintenance mainly limits vegetation to
249 herbaceous plants and tree and shrub seedlings.

250 The abundance-dominance of plant species were estimated using the Londo decimal scale
251 (Londo, 1976). For unknown species, plant vouchers were collected in the field and
252 subsequently were identified using Flora Iranica (Rechinger, 1963), Flora orientalis (Boissier,
253 1867), and Flora of Iran (Assadi et al., 1989), then stored in the herbarium of the Faculty of
254 Natural Resources at the University of Tehran.

255 Indicator Species Analysis was applied to identify species indicative of cut and fill slopes
256 following the method outlined by De Cáceres and Legendre (2009). This method is useful to
257 identify species that are strongly associated with specific environmental conditions, habitats,
258 or ecological changes. The abundance-dominance values were used to calculate indicator
259 values. This value reflects how strongly a species is associated with cut or fill slope. To
260 determine the statistical significance of indicator species, 999 permutations were conducted
261 using the "indicspecies" package in R (version 3.6.1; R Core Team, 2021). Further root
262 measurements and computations of species importance values were exclusively performed
263 for the indicator species identified through the Indicator Species Analysis.

264 **2.3. Species Importance Value (SIV)**

The Species Importance Value (SIV) is a dimensionless ecological index used to heuristically represent the dominance of a species within a community based on its relative species density, relative species frequency, relative aboveground coverage and relative underground coverage by roots parameters (Hao et al., 2021). The rationale behind using this index is that dominant species are more successful in the community and better adapted to the environmental conditions. SIV is calculated as follows (Hao et al., 2021):

$$SIV = D_R + F_R + C_{RA} + C_{RU} \quad (1)$$

where for a specific indicator species in an inventoried plot area (in m^2) D_R is the dimensionless relative species density, F_R is the dimensionless relative species frequency, C_{RA} is the dimensionless relative aboveground coverage by the projected area of foliage (abundance-dominance), and C_{RU} is the dimensionless relative underground coverage by roots. Each of these four parameters is calculated as follows:

$$\boldsymbol{D_R = \frac{\sum_{i=1}^{n} D_i}{\sum_{i=1}^{n} N_p^i} \times 100} \quad (2)$$

$$\boldsymbol{F_R = \frac{\sum_{i=1}^{n} F_i}{\sum_{i=1}^{n} F_s^i} \times 100} \quad (3)$$

$$\boldsymbol{C_{RA} = \frac{C_A}{\sum_{i=1}^{n} C_A} \times 100} \quad (4)$$

$$\boldsymbol{C_{RU} = \frac{C_U}{\sum_{i=1}^{n} C_U} \times 100} \quad (5)$$

Where n is the numeration of each different indicator species i to n = 13, C_A is the abundance-dominance value estimated by Londo decimal scale (Londo, 1976), and C_U is the root area (in m^2), determined by measuring the projected horizontal area of the root system,

which was secured to a needle board. On an inventoried plot, relative species density D_R and relative frequency F_R depend on the dimensionless density D_i of an individual species and the dimensionless species frequency F_i as follows:

$$\boldsymbol{D_i} = \frac{\boldsymbol{N_s^i}}{\sum_{\boldsymbol{i=1}}^{\boldsymbol{n}} \boldsymbol{N_s^i}} \tag{6}$$

$$\boldsymbol{F_i} = \frac{\boldsymbol{N_p^i}}{\sum_{\boldsymbol{i=1}}^{\boldsymbol{n}} \boldsymbol{N_p^i}} \tag{7}$$

Where N_s^i is the number of the *i*-th indicator species observed within the boundaries of an inventoried plot and N_p^i is the number of plots colonized by the *i*-th indicator species.

2.4. Plant Characteristics and Biomechanical Properties

To calculate the species importance value, the height (in m) of aboveground indicator plants was measured and the intact root systems of 65 sample plants (5 samples for each of 13 indicator species) were excavated with the surrounding soil intact using metal cores to determine root depth and spread in the laboratory. Initial trial-and-error excavation typically revealed that the maximum spread of the roots of an individual plant closely mirrored the projection of the crown, and the maximum rooting depth was approximately 0.3 m. The soil core sampling method was used to excavate each root system of sample plants (Smit et al., 2013). The soil core sample has a diameter of 0.15 m and a height of 0.30 m. The cores were arranged such that the stems were centrally located within them. None of the collected root systems extended beyond the plot boundaries. After collecting each root system, the core holes were carefully refilled, ensuring no visible signs remained from the excavation.

Each of the 65 root systems was packed in foam boxes with ice packs following the protocol by Zhang et al. (2019) and transferred to the laboratory within two to three days. In the laboratory, we used the needle-board technique (Smit et al., 2013) to hold and fix the flexible

roots in the approximate in-situ position during the gentle washing with low-pressure water to minimize damage and reduce loss of finer roots (Smit et al., 2013). The needle board held the largely soil-free roots in three vertical layers marked at depths of 0.0-0.1 m, 0.1-0.2 m, and 0.2-0.3 m. The majority of indicator species exhibited fibrous root systems, with the exception of tree seedlings, which possessed a taproot system. Each root system was carefully inspected from the roots of other plants, using connectivity, color, texture, and overall appearance of the roots in the delineation.

This study employed a visual enumeration technique at a magnification of 10X to count the roots across the three distinct layers (0.0-0.1 m, 0.1-0.2 m, and 0.2-0.3 m). Root branching was considered during the enumeration process, with branched roots being recorded as distinct entities. In addition, this study measured root diameter (in mm) and length (in mm) to estimate root volume (in mm^3) and root density (in percentage) in each of the three layers. The measurement of root length was conducted using a steel ruler, which provided an accuracy of 1 mm. In contrast, the diameter of the roots was assessed utilizing a digital vernier caliper, offering a precision of 0.01 mm.

Following the completion of measurements regarding root density and distribution, this study proceeded to collect 10–20 root samples from each of the 65 root systems randomly, resulting in a total of 442 replicates. In the sample selection process, we aimed to ensure adequate representation across all diameter ranges. Tensile root samples were approximately 0.15 m long (grip-to-grip distance), consisting of relatively straight, untwisted root segments that underwent a visual inspection to confirm the absence of decay or injuries. The selected root segments were trimmed at the ends with sharp scissors, placed in individual plastic bags, and sprayed with a 15 percent alcohol solution to prevent fungal and microbial degradation. Each carefully sealed bag was stored in a refrigerator at 4 °C to maintain the in-situ root tensile strength until testing within 48 hours (Vergani et al., 2012).

To measure root maximum tensile force, this study used a Universal Testing Machine (SANTAM Co. SMT-5, Tehran, Iran). The tests were conducted at a speed of 10 mm min^{-1} until rupture occurred, typically in the midsection of the roots (at 0.07 m to 0.08 m). Samples that exhibited rupture close to the clamps were excluded from further analysis. Further, power-law approximations were fitted to establish two empirical relationships between root diameter d_i (in mm) for each indicator species i = 1 to n = 13 versus (1) maximum tensile force F_{max} (in N) for each of the 13 indicator species i and (2) modulus of elasticity E (in MPa) as follows

$$\boldsymbol{F_{max(d_i)} = F_0 \left(\frac{d_i}{d_0}\right)^{\xi}} \quad (8)$$

$$\boldsymbol{E(d_i) = E_0 \left(\frac{d_i}{d_0}\right)^{\beta}} \quad (9)$$

where F_0 (in N) and E_0 (in MPa) are scaling factors, while ξ and β are dimensionless empirical exponents, respectively, and d_0 is the reference root diameter (expressed as 1 mm).

2.5. Root Bundle Model with Weibull Survival Distribution

The Root Bundle Model with a Weibull survival distribution is a fiber bundle model developed to estimate maximum root tensile force as a function of root diameter distribution (Schwarz et al., 2013). The Root Bundle Model with a Weibull survival distribution was developed to estimate the force required to pull roots from the soil. This force reflects the root's resistance to being completely extracted from the soil, which occurs after the root has experienced rupture. The model also calculates the probability of root failure by using Weibull survival distribution, based on laboratory measurements of maximum tensile force or field pullout tests. In this study, laboratory tests were used to assess the tensile force required to cause root rupture for different root diameters, providing a more accurate

understanding of root-soil interactions. Based on root spatial distribution, diameter, maximum tensile force, and elastic modulus, the total cohesive strength of root reinforcement (c_r in Pa) for steep slope stability is:

$$\boldsymbol{c_r = \sum_{i=1}^{n} F(d_i, \Delta x)\, S(\Delta x^*)} \tag{10}$$

where i = 1 to n represents the numeration of roots passing the shear surface, F is the tensile force (in N) resisted by each root, Δx signifies the displacement unit (in mm), and S denotes the Weibull survival distribution (dimensionless). The two-parameter Weibull survival distribution, as a function of the normalized root displacement Δx^* (normalized by the maximum displacement Δx_{max}^{fit}, in mm) is:

$$\boldsymbol{S(\Delta x^*) = \exp\left[-\left(\frac{\Delta x^*}{\lambda}\right)^{\omega}\right]} \tag{11}$$

where λ and ω are the dimensionless empirical scale and shape parameters of the Weibull survival distribution, respectively. The normalized displacement Δx^* for each root diameter d_i is:

$$\boldsymbol{\Delta x^*(d_i) = \frac{\Delta x}{\Delta x_{max}(d_i)}} \tag{12}$$

where $\boldsymbol{\Delta x_{max}}$ is the maximum observed displacement (in mm). Maximum tensile force of the single root can be calculated as:

$$\boldsymbol{F(d_i, \Delta x) = \frac{\pi . E_0}{4 . L_0} . d_i^{2+\beta-\alpha} \qquad F(d_i, \Delta x) < F_{max(d_i)}} \tag{13}$$

Where L_0 (in mm) serves as a scaling factor estimated by an empirical power law approximation that correlates the root length L (in mm) and the diameter, and α is a dimensionless empirical power–law exponent.

$$\boldsymbol{L(d_i) = L_0 \left(\frac{d_i}{d_0}\right)^{\alpha}} \quad (14)$$

2.6. Estimation of Roadside Slope Stability

This study used the Probabilistic Multidimensional Shallow Landslide Analysis to estimate the probability of shallow landslide occurrence and the effective contribution of the indicator species to forest roadside (i.e. cut and fill slopes) for slope stabilization. This model is based on the pioneering three-dimensional slope stability model (Terwilliger and Waldron, 1991) and on the more recent Multidimensional Shallow Landslide Model (Dietrich et al., 2007; Milledge et al., 2014). The Probabilistic Multidimensional Shallow Landslide Analysis seamlessly integrates the three-dimensional equilibrium of forces with Monte Carlo simulation to address the uncertainty of the specified parameters. The equilibrium of forces is applied at the centroid of a hypothetical parallelepiped landslide mass where the groundwater level remains constant and parallel to the undisturbed slope surface, simulating both saturated and unsaturated soil and thus neglecting infiltration, evapotranspiration, suction, and capillary rise. The Probabilistic Multidimensional Shallow Landslide Analysis simulates the effect of both basal and lateral root reinforcement (Equation 10) on steep slopes, broadening the applicability of slope stability simulations. The dimensionless ratio (Ω) of soil-root cohesive forces to the downslope component of the weight of the potential landslide mass due to gravity:

$$\boldsymbol{\Omega = \frac{F_{rb} + 2F_{rl} + F_{rd} + F_{ru} - F_{du}}{F_{dc}}} \quad (15)$$

where F_{rb} (in N) is the resisting soil-root cohesive force acting at the basal plane of failure, e.g., at a soil–bedrock boundary; F_{rl} (in N) is the soil-root cohesion acting on the two parallel sides of the block; F_{rd} (in N) is the soil-root cohesion at the central block from the downslope edge; F_{ru} (in N) is the lateral root reinforcement acting on the upslope side of the parallelepiped; F_{du} (in N) is the active force of gravity acting on the parallelepiped from the upslope edge; and F_{dc} (in N) is the soil weight and vegetation surcharge force acting downslope. A comprehensive description of all equations and parameter ranges of each component of Equation 15 can be found in the Supplementary Materials and in Cislaghi et al. (2017, 2018).

2.7. Statistical Analysis

This investigation determined the normality and homogeneity of observations of root diameter, number of roots, root volume, root length, plant height, and root maximum tensile force using the Shapiro-Wilk normality test and the Levene test, respectively. As the observations did not conform to a normal distribution (significance level of 0.05), logarithmic or Box-Cox transformations were applied to the data. Root maximum tensile force was normalized logarithmically, whereas root diameter, number of roots, root volume, root length, plant height was normalized by the Box-Cox transformation, respectively. Significant differences in plant and root characteristics and root maximum tensile force at a significance level of 0.05 were determined by analysis of variance and post-hoc comparisons using the Tukey honestly significant differences test (hereafter Tukey test). All statistical analyses in this study were performed using the R software, version 3.6.1 (R Core Team, 2021).

3. Results

3.1. Indicator Species of fill and cut slopes

400 Out of the 85 species identified on the cut and fill slope in the Namkhane district (listed in
401 the Supplementary Material Table S1), 13 species were selected as indicators based on
402 Indicator Species Analysis. Of these, 9 species (69 percent) were primarily found on the cut
403 slopes, while 4 species (31 percent) were associated with the fill slopes (Table 1). The 9 tree
404 and shrub seedlings, as well as the herbaceous species on the cut slopes, included the
405 following: (1) *Carpinus betulus* (tree seedlings), (2) *Rhamnus frangula* (seedlings), (3)
406 *Fagus orientalis* (tree seedlings), (4) *Athyrium filix-femina,* (5) *Acer cappadocicum* (tree
407 seedlings), (6) *Epimedium pinnatum*, (7) *Pteris cretica,* (8) *Hypericum androsaemum,* and
408 (9) *Hypericum perforatum*. The indicator species on the fill slopes were all herbaceous and
409 included the following: (1) *Sambucus ebulus*, (2) *Geum urbanum*, (3) *Setaria glauca*, and (4)
410 *Phyllitis scolopendrium*. Nine species on both cut and fill slopes were classified as native,
411 three were potentially invasive, and one was invasive (Table 1). Among the 13 indicator
412 species growing on the 116 inventoried plots, *S. ebulus* had the largest relative density D_R
413 (50.4 percent), while *H. perforatum* had the smallest D_R (3.4 percent). The indicators *G.*
414 *urbanum* and *P. cretica* had the largest and smallest relative frequencies F_R, respectively.
415 The largest relative coverage aboveground C_{RA}, and belowground C_{RU}, and thus the largest
416 *SIV* was estimated for the native fern *A. filix-femina*. Remarkably, each of the 13 indicator
417 species occurred either on the cut slope or the fill slope, but not on both.

Table 1. Species importance value (*SIV*) for 13 selected indicator species on cut and fill slopes based on relative species density (D_R), relative frequency (F_R), relative aboveground coverage (C_{RA}), and relative underground coverage (C_{RU})

Slope	Species	Status[†]	ISA Statistic[††]	D_R (%)	F_R (%)	C_{RA} (%)	C_{RU} (%)	*SIV* (%)
Cut slope	*Carpinus betulus* L. (seedling)	Native (Sabeti, 1976)	0.4***	41.0	31.8	29.9	24.1	126.8
	Rhamnus frangula L. **(**seedling**)**	Native (Sabeti, 1976)	0.2***	7.7	9.9	27.6	34.5	79.7
	Fagus orientalis Lipsky. (seedling)	Native (Sabeti, 1976)	0.3***	23.6	23.5	13.9	11.8	72.8
	Athyrium filix-femina (L.) Roth.	Native (Rechinger, 1978)	0.3**	39.5	35.2	70.1	36.4	181.2
	Acer cappadocicum Gled. (seedlins)	Native (Sabeti, 1976)	0.3**	18.0	34.9	28.7	29.6	112.1
	Epimedium pinnatum Fisch. ex DC.	Native (Rechinger, 1978)	0.2**	7.7	7.8	2.3	11.0	28.7
	Pteris cretica L.	Native (Eyvazi, 2014)	0.2*	46.36	0.08	18.82	33.68	98.93
	Hypericum androsaemum L.	Potentially invasive (Shakeri et al., 2012)	0.2*	46.4	40.6	7.1	16.3	110.4
	Hypericum perforatum L.	Invasive (Shakeri et al., 2012)	0.1*	3.4	8.6	1.7	4.7	18.4
Fill slope	*Sambucus ebulus* L.	Potentially invasive (Shakeri et al., 2012)	0.5***	50.4	38.1	34.5	35.3	158.3
	Geum urbanum L.	Native Pioneer (Rechinger, 1978)	0.3***	34.3	41.5	22.8	14.0	112.6
	Setaria glauca (L.) P.Beauv.	Potentially invasive (Shakeri et al., 2012)	0.2*	2.7	5.1	11.3	20.4	39.4
	Phyllitis scolopendrium (L.) Newman.	Native (Eyvazi, 2014)	0.2*	9.3	15.3	31.5	30.3	86.3

[†] Pioneer species refers to plants that are the first to colonize newly disturbed habitats (Dalling, 2008). Native species are either indigenous or endemic to the Hyrcanian Forests. Invasive plants are a subset of naturalized species with the potential to spread and reproduce away from their origin (Inderjit, 2005). Potentially invasive species are native to some parts of the Hyrcanian Forest but have the potential to spread beyond their original range.

[††] The Indicator Species Analysis statistic is calculated from a permutational test. A higher statistic indicates a stronger association between a species and a microhabitat, such as a cut or fill slope. Asterisks indicate statistical significance at the following levels: 95 percent (*), 99 percent (**), and 99.9 percent (***).

3.2. Root Characteristics

The number of roots significantly varied among the indicator species ($\mathcal{F}$ = 22.53, probability < 1E-15; Figure 2). *C. betulus* seedlings, *R. frangula* seedlings, *F. orientalis* seedlings, *A. cappadocicum* seedlings, *H. perforatum*, *G. urbanum*, and *S. glauca* had the lowest root abundance (Figure 2), suggesting relatively fewer roots within their root systems. The Tukey test showed that *A. filix-femina* and *P. cretica* on the cut slope and *P. scolopendrium* on the fill slope had significantly more abundant roots compared to *C. betulus* seedlings, *R. frangula* seedlings, *F. orientalis* seedlings, *A. cappadocicum* seedlings, *H. androsaemum*, and *H. perforatum* on the cut slope as well as *S. ebulus*, *G. urbanum*, and *S. glauca* on the fill slope.

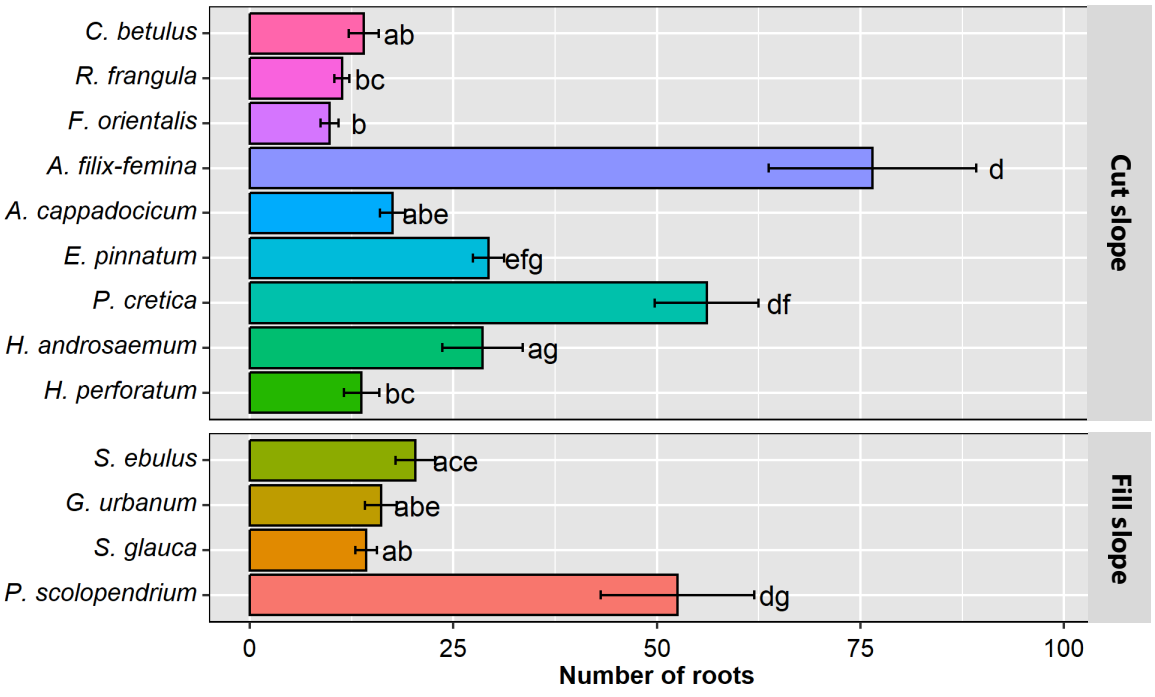

Figure 2. The average number of roots collected within a cylindrical core volume of 785000 mm^3 was measured for five plants of each of the 13 indicator species found on either the cut or on fill slopes. Columns sharing the same lowercase letters indicate that the number of roots is not statistically different at a significance level of 0.05.

The analysis of variance revealed significant differences in root volume among groups of the 13 species ($\mathcal{F}$ = 33.68, probability < 1E-15; Figure 3). Post-hoc analysis using the Tukey test

indicated that the root volume of *S. ebulus* (733 mm^3), *A. filix-femina* (549 mm^3), *P. cretica* (507 mm^3), *H. androsaemum* (385 mm^3), and *G. urbanum* (239 mm^3) were not significantly different. In contrast, the root volume of *S. glauca* (8 mm^3) was significantly smaller than that of the other 12 indicator species.

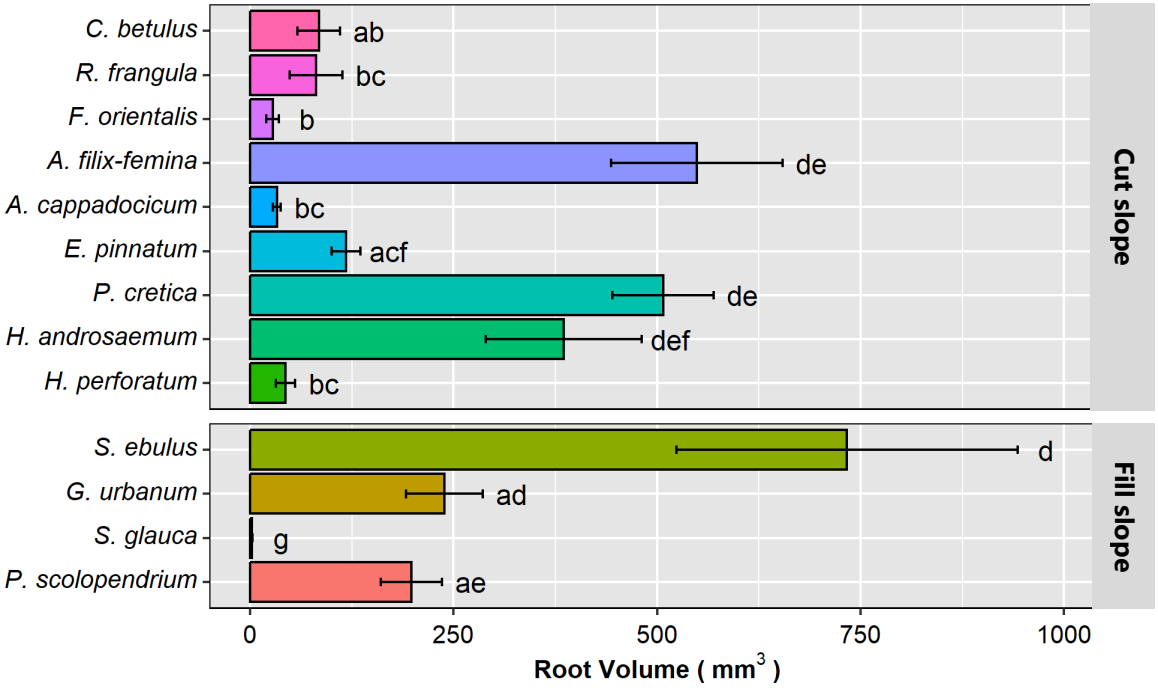

Figure 3. Average root volume for five plants of each of the 13 indicator species within the cylindrical core volume of 785000 mm^3. Columns sharing the same lowercase letters indicate that the number of roots is not statistically different at a significance level of 0.05.

Based on the five plant specimens collected for each indicator, Figure 4 shows that, except for the potentially invasive *S. ebulus*, all seven other herbaceous indicator species did not significantly extend roots deeper than 0.1 m. On fill slopes, 11 percent of the large roots of *S. ebulus* significantly penetrated to depths between 0.2 m and 0.3 m, consistent with the root distribution of the five indicators found exclusively on cut slopes. These include native tree seedlings of *C. betulus* (13 percent of the root distribution), native shrub seedlings of *R. frangula* (13 percent), native tree seedlings of *F. orientalis* (6 percent), native tree seedlings of *A. cappadocicum* (10 percent), and potentially invasive plants of *H. androsaemum* (11

percent). The other three indicators found on fill slopes were restricted to rooting within the top 0.1 m of soil: *G. urbanum* (100 percent of roots), *S. glauca* (100 percent), and *P. scolopendrium* (100 percent). Indicator species on cut slopes *A. filix-femina* (96 percent), *E. pinnatum* (100 percent), and *P. cretica* (93 percent), did not extend below 0.2 m in depth.

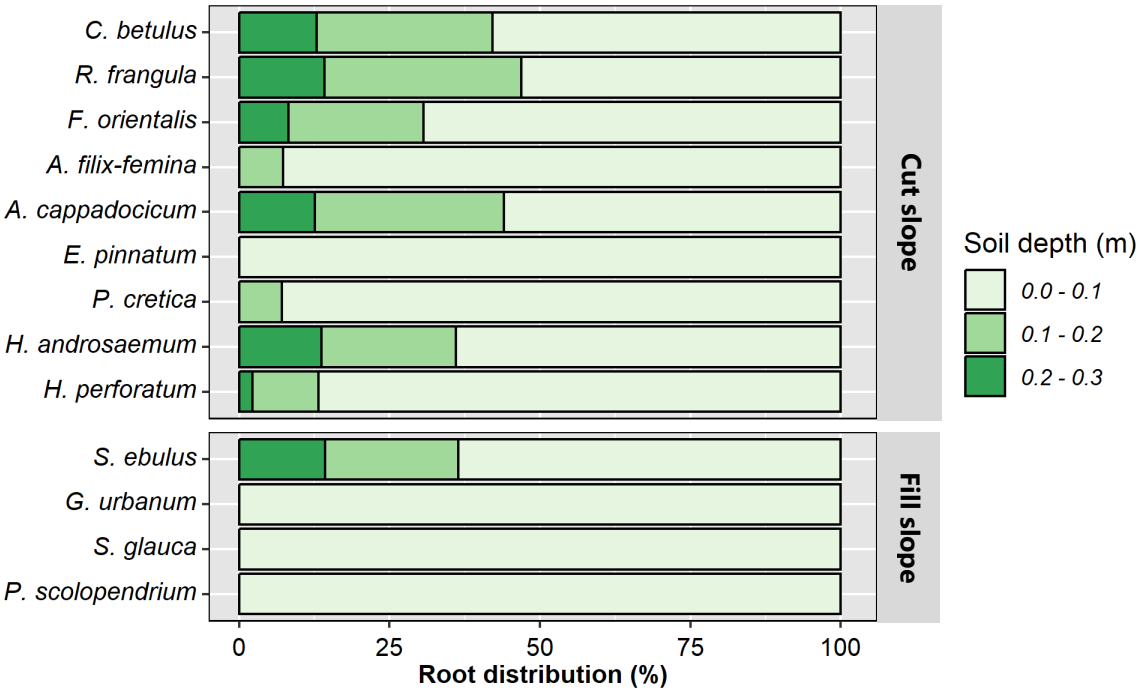

Figure 4. Average root distributions across three soil depths (0.0 m to 0.1 m, 0.1 m to 0.2 m, and 0.2 m to 0.3 m) measured for five plants of each of the 13 indicator species.

3.3. Indicator Aboveground Characteristics

As determined in this study by analysis of variance ($\mathcal{F}$ = 20.34, probability < 1E-15), the fern *A. filix-femina* with a mean plant height of 0.64 m was significantly taller than all the other 12 indicator species (Figure 5).

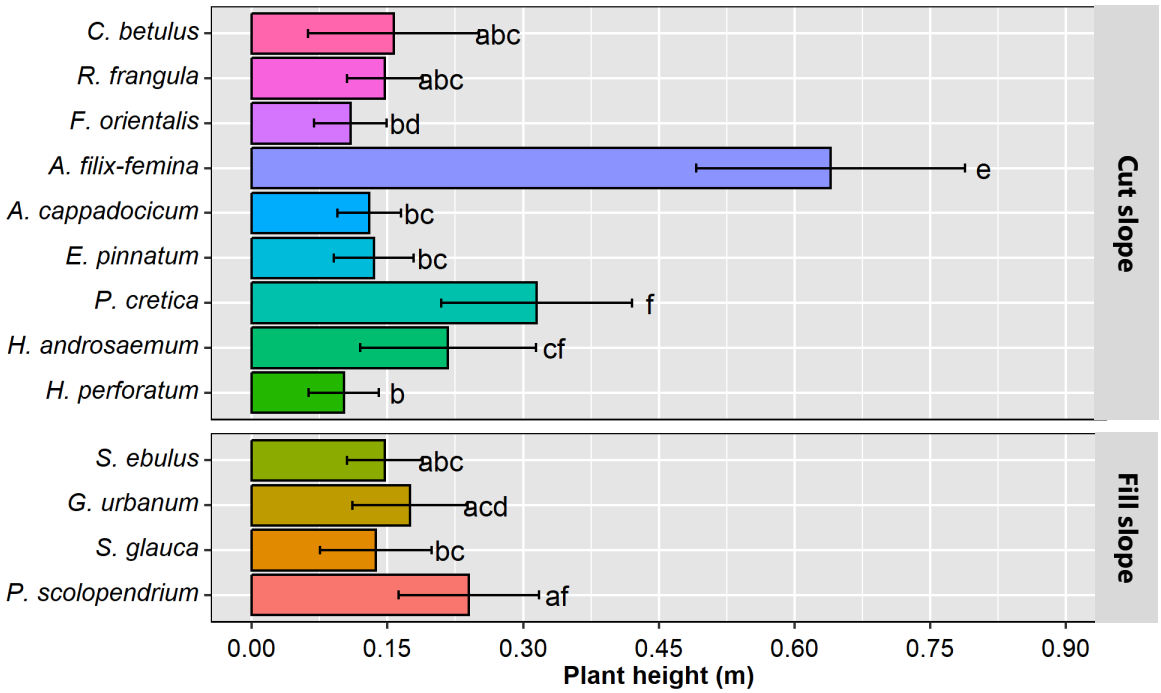

Figure 5. Indicator species height. Means sharing the same lowercase letters are not statistically different at a significance level of 0.05.

3.4. Root Mechanical Characteristics

The ranges of measured root diameters (0.01 to 5.03 mm) from core samples of 65 root systems were small for all 13 indicators except *S. ebulus*, falling into the fine root classifications of < 2 mm. In the Supplementary Materials, Figure S3 shows the empirical relationship between measured root diameter and measured maximum root tensile force. The mean maximum tensile force at root rupture ranged from 2.4 N for *G. urbanum* to 16.4 N for *S. ebulus* (Table 2). The root modulus of elasticity ranged between a minimum of 1.4 MPa and a maximum of 955 MPa, with the roots of *S. glauca* (124 MPa) on average being stiffer compared to other species, while the roots of *S. ebulus* (7.1 MPa) were the least stiff among all 13 indicators.

The root modulus of elasticity ranged between a minimum of 1.4 MPa and a maximum of 955 MPa, with the roots of *S. glauca* (124 MPa) on average tending to be more elastic, while the roots of *S. ebulus* (7.1 MPa) on average tended to be less elastic among all 13 indicators.

Table 2. Minimum, mean and maximum root diameter, maximum tensile force, and root modulus of elasticity for each indicator species

Slope	Species	Diameter (mm)			Maximum tensile force (N)			Modulus of elasticity (MPa)		
		Min.	Mean	Max.	Min.	Mean	Max.	Min.	Mean	Max.
Cut slope	*Carpinus betulus* L. (seedling)	0.12	0.59	1.45	1.2	8.7	42.6	7.7	40.8	371.4
	Rhamnus frangula L. (seedling)	0.09	0.63	1.90	0.4	7.2	51.1	4.9	24.6	103.6
	Fagus orientalis Lipsky. (seedling)	0.14	0.61	1.61	0.9	10.4	46.4	2.1	28.1	88.1
	Athyrium filix-femina (L.) Roth.	0.08	0.36	0.86	0.9	3.8	11.2	1.4	54.6	220.0
	Acer cappadocicum Gled. (seedling)	0.09	0.43	1.43	0.6	3.9	31.8	10.3	27.6	94.3
	Epimedium pinnatum Fisch. ex DC.	0.06	0.36	0.65	0.4	3.0	8.0	3.0	44.7	353.7
	Pteris cretica L.	0.04	0.33	0.75	0.7	3.7	7.8	8.2	77.0	955.0
	Hypericum androsaemum L.	0.15	0.70	1.58	0.4	6.1	20.0	2.0	20.2	89.1
	Hypericum perforatum L.	0.06	0.46	1.03	0.4	2.9	13.7	4.5	27.7	141.5
Fill slope	*Sambucus ebulus* L.	0.46	1.75	5.39	1.2	16.4	58.0	2.5	7.1	18.5
	Geum urbanum L.	0.18	0.54	1.26	0.7	2.4	6.0	2.0	12.6	31.6
	Setaria glauca (L.) P.Beauv.	0.08	0.22	0.81	0.5	2.8	8.7	1.6	124	557.0
	Phyllitis scolopendrium (L.) Newman.	0.10	0.36	0.60	0.6	2.5	8.5	2.7	36.0	160.1

Note: Root diameter measurements were recorded to the nearest 0.01 mm, maximum tensile force to the nearest 0.1 N, and modulus of elasticity to the nearest 0.1 MPa.

3.5. Root Reinforcement

Table 3 presents the key parameters for the Root Bundle Model utilizing a Weibull survival distribution, selected in this study to estimate slope reinforcement provided by the 13 indicator species. The parameters include the scaling factors (F_0, E_0, and L_0), exponents (ξ, β, and α), and Weibull coefficients (λ and ω). The F_0 ranged from 4.3 N to 20.1 N, E_0 from 26.2 MPa to 186.5 MPa, and L_0 from 2 mm to 12 mm. The minimum values for the dimensionless exponents ξ, β, and α and for the Weibull scale parameter λ, and shape parameter ω were 0.5, -1.8, -1.4, 1.0, and 1.4, respectively. The maximum values for these parameters were 2.2, -0.4, 1.7, 1.2, and 4.3, respectively. Further details are available in Figure S3 in Supplementary Materials.

Table 3. Parameters for the Root Bundle Model with a Weibull survival distribution for each 415 indicator species, including the nominal tensile force F_0, nominal modulus of elasticity

500 (E_0), nominal length (L_0), dimensionless empirical exponents (ξ, β, and α), and Weibull
501 coefficients λ and ω to define the survival distribution for each indicator species
502

Slope	Species	F_0 (N)	E_0 (MPa)	L_0 (mm)	ξ	β	α	λ	ω
Cut slope	*Carpinus betulus* L. (seedling)	18.9	186.5	5.7	1.9	-0.8	-0.11	1.1	2.9
	Rhamnus frangula L. (seedling)	12.0	146.3	3.9	2.2	-0.6	-0.4	1.1	1.7
	Fagus orientalis Lipsky. (seedling)	20.1	37.7	3.0	2.1	-0.5	0.8	1.0	2.1
	Athyrium filix-femina (L.) Roth.	8.8	35.4	8.6	0.8	-1.2	1.7	1.1	2.0
	Acer cappadocicum Gled. (seedling)	15.2	113.4	5.9	2.0	-0.7	-0.4	1.1	2.5
	Epimedium pinnatum Fisch. ex DC.	7.7	64.6	5.0	1.0	-1.0	0.9	1.2	2.0
	Pteris cretica L.	6.2	40.8	6.0	0.4	-1.4	1.4	1.1	2.4
	Hypericum androsaemum L.	9.0	47.7	11.6	1.2	-0.9	-0.3	1.1	2.1
	Hypericum perforatum L.	7.6	33.5	9.8	1.4	-1.1	-0.5	1.1	1.9
Fill slope	*Sambucus ebulus* L.	9.1	57.3	1.9	1.1	-0.4	0.4	1.1	1.8
	Geum urbanum L.	4.3	33.5	7.4	0.9	-1.0	-0.2	1.1	1.6
	Setaria glauca (L.) P.Beauv.	6.1	34.1	8.5	0.5	-1.8	-1.4	1.1	4.3
	Phyllitis scolopendrium (L.) Newman.	4.6	26.2	7.9	0.6	-1.5	0.6	1.1	1.4

503 The analysis of variance for root reinforcement (Equation 10) showed significant differences
504 among some groups of indicator species ($\mathcal{F}$ = 38.39, probability < 1E-15). However, on both
505 the cut and fill slopes, insignificant differences were observed among all nine species on the
506 cut slopes and all four herbaceous species on the fill slopes. The root reinforcement from
507 native herbaceous *A. filix-femina* (4538 Pa) and *P. cretica* (4513 Pa) was significantly larger
508 than that of the other six indicators collected on cut slopes but were not significantly different
509 from the root reinforcement of native herbaceous *E. pinnatum* (Figure 6). This study found
510 that native herbaceous *P. scolopendrium* and potentially invasive *S. ebulus,* provideed
511 significantly more root reinforcement than the invasive *S. glauca* on fill slopes (Figure 6).

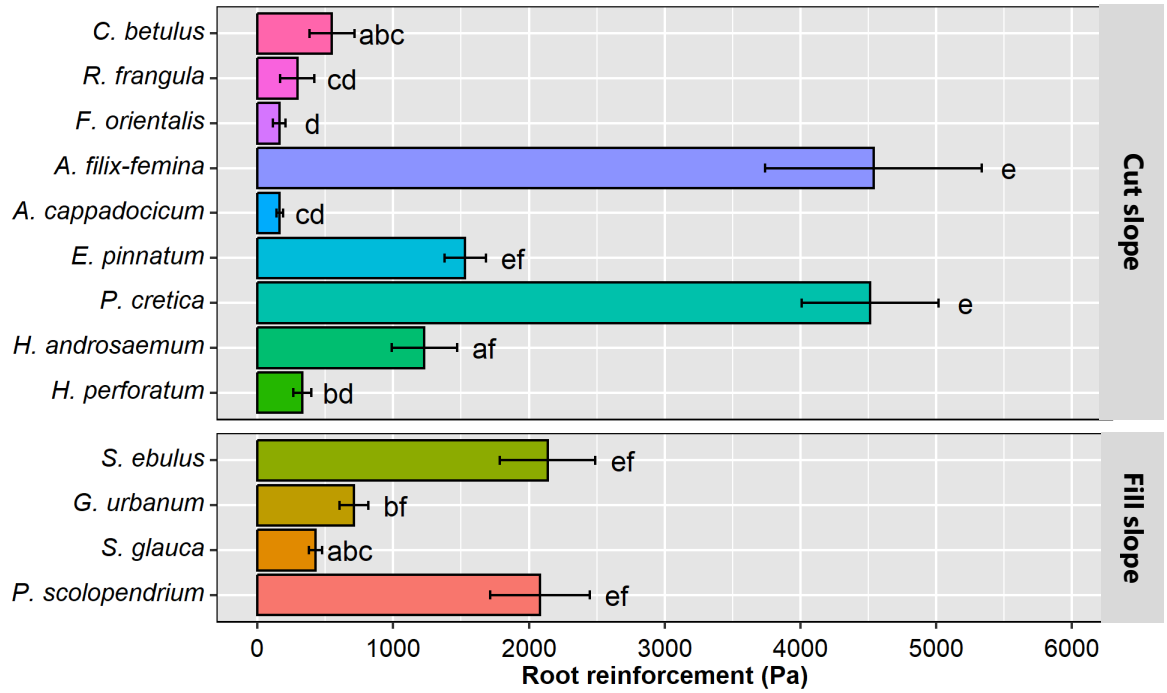

Figure 6. Root reinforcement of 13 indicator species. Means sharing the same lowercase letters are not statistically different at a significance level of 0.05.

3.6. Slope Stability Estimates

Based on both basal and lateral root reinforcement (Equation 10), this study identified *A. filix-femina* and *P. cretica* as the most effective native indicators for significantly stabilizing cut slopes in the Namkhane district of the Kheyrud Forest. Figure 7 shows that the probability of slope instability is 50 percent for the steep slopes radiating outward from the edge of the gravel roadbed. The probabilities of slope instability for species on cut slopes were as follows: *A. cappadocicum* (45 percent), *A. filix-femina* (7 percent), *C. betulus* (38 percent), *E. pinnatum* (23 percent), *F. orientalis* (45 percent), *H. androsaemum* (28 percent), *H. perforatum* (41 percent), *P. cretica* (4 percent), *R. frangula* (42 percent). On fill slopes, the probability of slope instability was 40 percent for *S. glauca*, 35 percent for *G. urbanum*, 18 percent for *P. scolopendrium*, and 17 percent for *S. ebulus* (Figure 7).

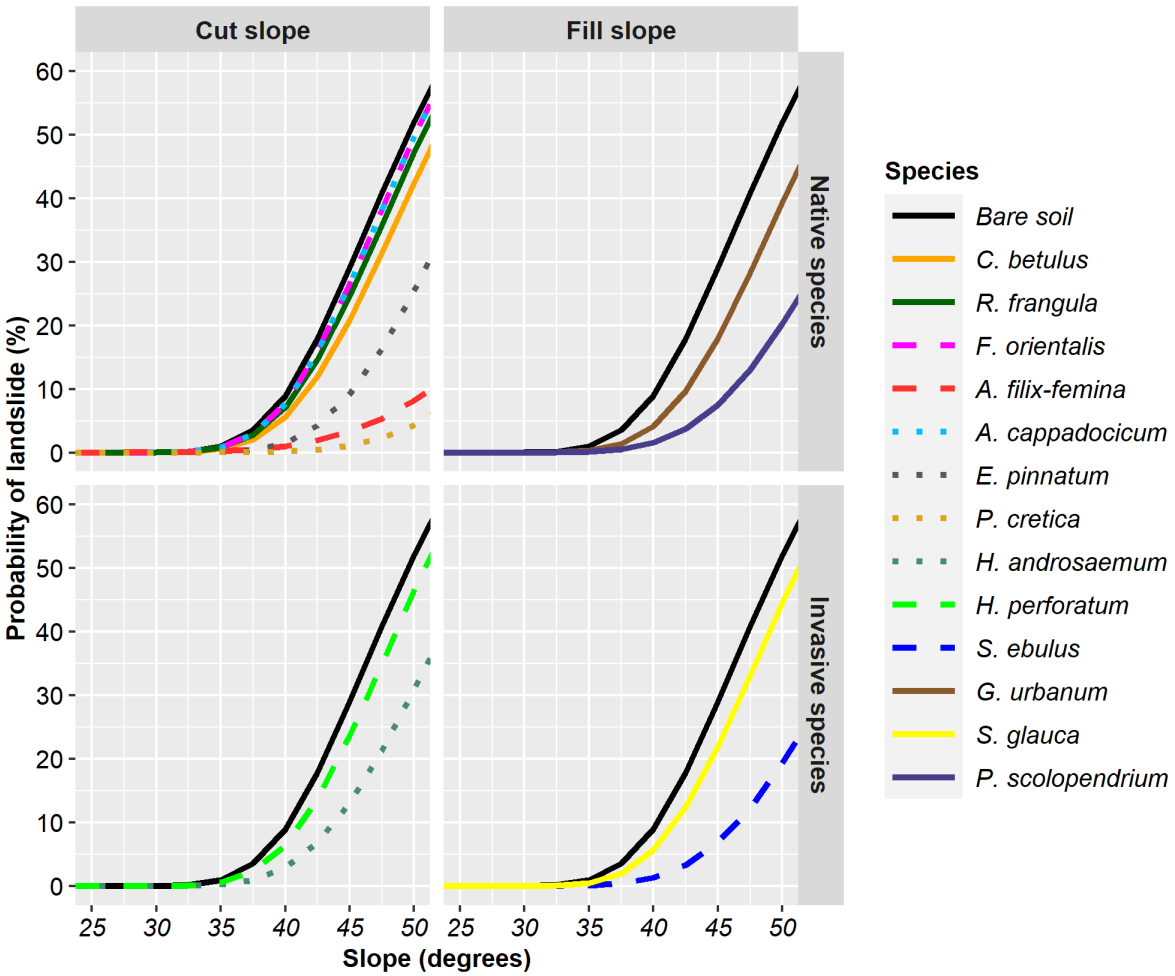

Figure 7. Estimated probability of steep cut or fill slope failure for the ratio (Ω) of soil-root cohesive forces to the downslope component of the gravitational weight of the potential landslide mass is less than 1, based on basal and lateral root reinforcement along the main forest gravel roads in the Namkhane district.

4. Discussion

This study found that two native ferns, *A. filix-femina* and *P. cretica*, growing on cut slopes, demonstrated significantly higher slope stabilization compared to most woody seedlings, even though their roots did not extend below 0.2 m into the soil. This indicates that despite shallow rooting, certain fern species can play a crucial role in enhancing slope stability, potentially due to their dense root mat or faster establishment on disturbed sites. The

assumption that the shear surface develops within the root-reinforced layer (0.0–0.3 m) is supported by field observations in the study area, where shallow landslides typically occur in the upper soil layers. However, applying a 3D slope stability model allows for the inclusion of not only the resistance provided by roots crossing the failure surface ("basal root reinforcement") but also the reinforcement acting along the margins of the potentially mobilizable soil mass ("lateral root reinforcement") (Dorren and Schwarz, 2016). Nevertheless, the inherent variability in root reinforcement—driven by tree characteristics (e.g., species, age, and density) and soil properties (e.g., geotechnical and hydrological parameters)—along with uncertainties regarding the mechanical response of roots (rupture or pullout), can influence slope stability assessments. This variability often leads to an overestimation of the stabilizing effects of vegetation, particularly when the failure plane extends into deeper soil layers. To improve the accuracy of these predictions, future research should prioritize the collection of site-specific, continuous monitoring data to validate and refine slope stability models. Root distribution, which refers to the spatial arrangement of roots within the soil profile across the soil layers (0.0-0.1 m, 0.1-0.2 m, and 0.2-0.3 m), is pivotal in estimating slope stabilization and is influenced by various key factors. In humid climates, roots tend to spread laterally from the stem quickly, but root lateral distribution decreases with increasing soil depth, especially for trees (Bischetti et al., 2009; Hytiris et al., 2015; Kokutse et al., 2016; Temgoua et al., 2016; Löbmann et al., 2020; Hao et al., 2023). Any decrease in root volume or biomass with depth is generally due to the high energy required to transport water and nutrients from deeper layers, reduced nutrient availability, limited soil aeration at depth, and less permeable geologic strata (Zhang et al., 2019; Deljouei et al., 2023). Typically, herbaceous roots are predominantly concentrated within the top 0.1 m to 0.2 m of soil (Burylo et al., 2011; Zhong et al., 2016) as observed in the Kheyrud Forest.

This study reveals significant variations in root characteristics, particularly root density, among the indicator species identified on cut and fill slopes. It is important to note that while some species exhibit adaptations that may aid in slope stabilization, others are merely surviving under challenging conditions, influenced by the road maintenance practices that prevent woody seedlings from maturing, such as regular mowing and cutting. These practices likely inhibit the growth of certain species, preventing them from reaching their full potential. Out of the 85 identified species, 13 have been highlighted as indicators of potential adaptation; however, further research is needed to distinguish between those that are thriving and those that are simply persisting (Saadati et al., 2023; Burylo et al., 2011). The distinct indicator species found on the cut and fill slopes in the Namkhane district highlight how these slopes differ in terms of environmental conditions, particularly soil characteristics, moisture retention, and disturbance levels. The lower number of indicator species on fill slopes can be attributed to several factors such as: soil displacement and compaction disrupt natural soil structure and reduce fertility, hindering plant establishment. Additionally, hydrological disconnection reduces soil moisture, while lower nutrient content in fill soils further limits plant growth. These slopes are also more vulnerable to erosion and harsh conditions, creating unstable habitats. Furthermore, competition from fast-growing or invasive species, such as *S. ebulus*, suppresses the establishment of more diverse plant species, including indicator species (Shakeri et al., 2021).

Root density variations are partly influenced by environmental factors, including bulk density, moisture content, fertility (Gholami-Derami et al., 2021), as well as anthropogenic disturbances (e.g. soil compaction on road shoulders can limit root development in some species). While variations in root area ratio and depth are associated with species-specific genetic factors, and planting density, external physical factors, such as hard soil layers or bedrock can hinder deeper root growth, potentially compromising slope stability (Hamidifar

et al., 2018). This interplay of genetic, environmental, and anthropogenic factors underscores the complexity of vegetation growth on disturbed roadside slopes.

Taller plants, such as the perennial fern *A. filix-femina*, provided greater slope reinforcement compared to shorter indicator species. This result is consistent with findings from Saifuddin et al. (2015), who observed a positive correlation between plant height and soil shear strength in *Leucaena leucocephala* and *Peltophorum pterocarpum*, though their study focused on greenhouse monocultures rather than natural herbaceous understory. It is clear that the relationship between plant height and root depth does not always align the conventional view that taller plants provide better slope stabilization due to deeper roots. Based on the 13 selected indicators selected and the 116 plots, situated on road cut and fill slopes, our findings suggest an exception to this heuristic. Specifically, while *A. filix-femina* is taller than the other species and provides significant slope reinforcement, its roots—similar to those of *P. cretica*— are concentrated primarily in the top 0.0–0.1 m layer of soil. This pattern is also seen in five other herbaceous species, apart from *S. ebulus*, which exhibited deeper roots.

This study investigated the relationship between root diameter and maximum root tensile force, consistent with the findings of previous scientific literature (Bischetti et al., 2007; Vergani et al., 2012; Karimi et al., 2022). These variations may be attributed to differences in cellulose-to-lignin ratios, with smaller roots having higher cellulose content relative to lignin (Genet et al., 2005), or they may be linked to the chemical composition of root tissues (Ye et al., 2017). Several factors influence root tensile force, including the depth and direction of root growth. Ghestem et al. (2014) found that roots of *Bauhinia championii* growing below a depth of 0.3 m exhibited higher tensile force compared to those roots of the same plant at shallow depths. Dumlao et al. (2015) observed that the root tensile force of the grasses *Avena fatua* and *Triticum aestivum* increased with root age due to progressive lignification. Additionally, the root tensile strength of the grasses *Hordeum vulgare* and *Chrysopogon*

612 *zizanioides* decreased with increasing plant density, as demonstrated by Loades et al. (2010)
613 and Hamidifar et al. (2018), with further support from studies on the relationship between
614 root tensile strength and plant density in various grass species (e.g., Burylo et al., 2011;
615 Genet et al., 2008). Moreover, Stokes et al. (2010) indicated that the growth rate of fine roots
616 is influenced by multiple factors, including plant age, site-specific precipitation, and soil
617 physical and chemical properties, even soil temperature.
618 The fine roots of seven out of the eight herbaceous indicators were relatively shallow (< 0.1
619 m) compared with the roots of tree and shrub seedlings that had significant rooting depth
620 below 0.2 m. The eighth herbaceous indicator, the coarse-rooted *S. ebulus* was rooted
621 significantly deeper than 0.2 m and was not significantly different from the two ferns in fill
622 slope reinforcement. The two shallow-rooted ferns, *A. filix-femina* and *P. cretica*
623 significantly enhanced cut slope stability, consistent with findings from De Baets et al.
624 (2008) and Burylo et al. (2011), who also observed that dense, fine, fibrous roots create
625 substantial slope reinforcement. Hence, deeper soil layers may often lack reinforcement from
626 herbaceous vegetation (Hytiris et al., 2015; Kokutse et al., 2016). Beyond 0.1 m depth, root
627 reinforcement on cut slopes was provided by the indicator species listed by probability in
628 Table 1: *C. betulus*, *R. frangula*, *F. orientalis*, *A. cappadocicum*, and *H. androsaemum*. A
629 meta-analysis by Kim et al. (2017) indicated that woody vegetation is generally more
630 effective at reinforcing soil compared to herbaceous vegetation. Over decades, deeper and
631 more extensive tree rooting contributes to longer-term slope stability relative to perennial
632 herbaceous vegetation. The findings of this study demonstrate that perennial, native
633 herbaceous species *A. filix-femina* and *P. cretica* provide significantly greater root
634 reinforcement than 10 of the other 11 indicator species.
635 While root reinforcement models offer valuable insights into soil-root interactions, they also
636 have limitations. Semi empirical models, such as those based on power-law approximations,

provide useful approximations but often lack fundamental depth, especially when their reliability is constrained by limited calibration data and the absence of significance testing. Improving slope stability models requires the integration of specific root characteristics (such as root diameter, root tensile strength, and distribution) as well as site conditions (such as soil depth and moisture content). This study highlights the importance of these factors in enhancing slope stability on cut slopes, as they control the mechanics of root reinforcement and displacement, ultimately influencing failure mechanisms (Giadrossich et al., 2017). However, obtaining accurate data for these models poses its own challenges. In this study, root distribution was assessed by excavating root systems, with soil samples extracted using cores and roots separated through washing and sieving—a process that may unfortunately led to some root loss (Masi et al., 2021). While advanced techniques such as automated imaging analyses (Dowdy et al., 1998; Costa et al., 2000), portable minirhizotrons, and color scanner systems (Pan et al., 1998) exist, they are prohibitively expensive. Researchers have explored indirect methods (Masi et al., 2020), but these approaches are often time-consuming, invasive, or destructive. Additionally, due to economic and logistical limitations, in-situ tensile tests could not be conducted in the field. As a result, many parameters crucial for slope stability modeling, such as slope failure dimensions, had to be estimated from literature rather than measured directly, further complicating the development of reliable models.

5. Conclusion

This study demonstrates the effectiveness of native herbaceous species in stabilizing cut and fill slopes along gravel roads in a part of Hyrcanian Forest, Northern Iran. The use of soil-bioengineering techniques, particularly the strategic planting of selected indicator species, significantly reduces the risk of slope failure caused by road construction, especially in the early years when pioneering species are established. These species develop dense root systems that bind surface soils, mitigating erosion and providing immediate reinforcement to

vulnerable slopes. In the long term, integrating soil-bioengineering approach with natural forest succession is anticipated to further enhance slope stability. As deeper-rooted trees establish and mature, their expansive root systems will provide additional and deeper soil reinforcement, reducing the likelihood of landslides or other slope failures. This combination of short-term and long-term stabilization strategies offers a sustainable alternative to conventional slope stabilization methods. The study highlights that bioengineered forest cover not only stabilizes slopes but also enhances ecological resilience by promoting natural succession. Over the time, this approach can help restore disturbed areas to their natural state, or close to it, thereby enhancing biodiversity and improving forest health. Environmental factors such as soil type, and regional climate significantly influence the vegetation community and indicator species. Given the diversity of plant associations across the Hyrcanian Forest from West to East, variation in indicator species is expected. Consequently, the indicator species recognized in this research may be applicable to forests with similar ecological conditions. Additionally, this study presents a fundamental approach for integrating local indicator species into soil-bioengineering techniques for forest road management, which can be adapted to match the specific vegetation types found in different regions. Although our study focused on a 30-year-old road network, the results should be also applicable to newly constructed forest roads with similar ecological conditions. In fact, among the 13 indicator species, nine are native to the Hyrcanian region. Utilizing these native species to quickly stabilize new road slopes would have a lower economic and environmental impact on forest ecosystems compared to other traditional or grey solutions. In general, it can be concluded that the results are applicable to similar forest associations in the Hyrcanian Forest ecoregion and forests in Central and Eastern Europe, particularly where the Fagetalia sylvaticae order dominates mountainous areas (Ujházyová et al., 2021). However, due to significant climatic variations, disturbances, management practices, and road maintenance

techniques, further studies are necessary to assess the applicability of these findings in those regions. This underscores the importance of region-specific research to understand how local climatic conditions influence slope stabilization processes. In conclusion, soil-bioengineering techniques offer a viable, ecologically sustainable solution for slope stabilization, reducing the reliance on mechanical interventions and fostering resilient ecosystems along forest road networks.

CRediT authorship contribution statement

Soghra Keybondori: Conceptualization, Methodology, Field Work, Laboratory Work, Writing – review & editing. **Ehsan Abdi:** Supervision, Conceptualization, Methodology, Investigation, Writing – review & editing. **Azade Deljouei:** Methodology, Visualization, Formal analysis, Writing – original draft, Writing – review & editing, Advising. **Alessio Cislaghi:** Methodology, Visualization, Formal analysis, Writing – original draft, Writing – review & editing. **Zahed Shakeri:** Supervision, Methodology, Plant voucher determination, Writing – review & editing. **Vahid Etemad:** Supervision, Methodology, Plant voucher determination, Writing – review & editing.

Declaration of Competing Interest

The authors declare that they have no known competing financial interests or personal relationships that could have appeared to influence the work reported in this paper.

Funding

This work was supported by the Iran National Science Foundation [agreement 99016122].

References

Assadi, M., Ramak Maassoumi, A.A., Khatamsaz, M., 1989. *Flora of Iran*. Tehran: Ministry of Agriculture, Islamic Republic of Iran.

Assadoallahi, F. 2001. Plant associations in Hyrcanian region. In: *Management of Hyrcanian Forests*, pp. 323–343. Tehran, Iran: University of Tehran.

Bischetti, G.B., Chiaradia, E.A., Epis, T., Morlotti, E., 2009. Root cohesion of forest species in the Italian Alps. Plant Soil 324, 71–89.

Bischetti, G.B., Chiaradia, E.A., Simonato, T., Speziali, B., Vitali, B., Vullo, P., Zocco, A., 2007. Root strength and root area ratio of forest species in Lombardy (Northern Italy). In

Bischetti, G.B., De Cesare, G., Mickovski, S.B., Rauch, H.P., Schwarz, M., Stangl, R., 2021. Design and temporal issues in Soil Bioengineering structures for the stabilisation of shallow soil movements. Ecol. Eng. 169, 106309.

Boissier, P.E., 1867. *Flora Orientalis: sive, Enumeratio plantarum in Oriente a Graecia et Aegypto ad Indiae fines hucusque observatarum* (Latin), 5 vols. and Suppl. edited by Robert Buser, Genevae et Basileae, 88.

Bordoloi, S., Ng, C.W.W., 2020. The effects of vegetation traits and their stability functions in bio-engineered slopes: A perspective review. Engineering Geology, 275, p.105742.

Braun-Blanquet, J. 1913. Die Vegetationsverhältnisse der Schneestufe in den Rätisch-Lepontischen Alpen. Denkschr. d. Schweiz. Naturf. Ges, 48.

Burylo, M., Hudek, C., Rey, F., 2011. Soil reinforcement by the roots of six dominant species on eroded mountainous marly slopes (Southern Alps, France). Catena 84 (1-2), 70–78.

Cazzuffi, D., Corneo, A., Crippa, E., 2006. Slope stabilisation by perennial "gramineae" in Southern Italy: Plant growth and temporal performance. Geotechnical & Geological Engineering, 24, 429-447.

Cislaghi, A., Bordoni, M., Meisina, C., Bischetti, G.B., 2017. Soil reinforcement provided by the root system of grapevines: Quantification and spatial variability. Ecol. Eng. 109, 169–185.

Cislaghi, A., Rigon, E., Lenzi, M.A., Bischetti, G.B., 2018. A probabilistic multidimensional approach to quantify large wood recruitment from hillslopes in mountainous-forested catchments. Geomorphology 306, 108–127.

Cislaghi, A., Alterio, E., Fogliata, P., Rizzi, A., Lingua, E., Vacchiano, G., Bischetti, G.B. and Sitzia, T., 2021. Effects of tree spacing and thinning on root reinforcement in mountain forests of the European Southern Alps. Forest Ecology and Management, 482, p.118873.

Costa, C., Dwyer, L.M., Hamilton, R.I., Hamel, C., Nantais, L., Smith, D.L., 2000. A sampling method for measurement of large root systems with scanner-based image analysis. Agron. J. 92, 621–627.

Dalling, J.W., 2008. Pioneer species. In Encyclopedia of Ecology, Five-Volume Set (pp. 27792782). Elsevier Inc.

Davis, P.H., 1984. *Flora of Turkey*. Edinburgh University Press. Vol. 9. https://www.jstor.org/stable/10.3366/j.ctvxcrf2m

De Baets, S., Poesen, J., Reubens, B., Wemans, K., De Baerdemaeker, J., Muys, B., 2008. Root tensile strength and root distribution of typical Mediterranean plant species and their contribution to soil shear strength. Plant Soil 305, 207–226.

De Cáceres, M., Legendre, P., 2009. Associations between species and groups of sites: indices and statistical inference. Ecology, 90(12), 3566-3574.

Deljouei, A., Cislaghi, A., Abdi, E., Borz, S.A., Majnounian, B., Hales, T.C., 2023. Implications of hornbeam and beech root systems on slope stability: From field and laboratory measurements to modelling methods. Plant Soil 483 (1-2), 547–572.

Dezhban, A., Attarod, P., Zahedi Amiri, G., Grant Pypker, T., & Nanko, K., 2019. Fog precipitation and rainfall interception in a pure natural oriental beech (Fagus orientalis L.) stand in the Hyrcanian Forests, North of Iran. Forest and Wood Products, 72(2), 89-100.

Dietrich, W.E., McKean, J., Bellugi, D., Perron, T., 2007. The prediction of shallow landslide location and size using a multidimensional land-slide analysis in a digital terrain model. In Proceedings of the Fourth International Conference on Debris flow Hazards Mitigation: Mechanics, Prediction, and Assessment (DFHM-4), Chengdu, China;10–13.

Dorren, L.K.A., Schwarz, M., 2016. Quantifying the stabilizing effect of forests on shallow landslide-prone slopes, in: Renaud, F.G., Sudmeier-Rieux, K., Estrella, M., Nehren, U. (Eds.), Ecosystem-Based Disaster Risk Reduction and Adaptation in Practice. Springer International Publishing, Cham, pp. 255–270. https://doi.org/10.1007/978-3-319-43633-3_11

Dowdy, R.H., Smucker, A.J.M., Dolan, M.S., Ferguson, J.C., 1998. Automated image analyses for separating plant roots from soil debris elutriated from soil cores. Plant Soil, 200, 91–94.

Dumlao, M.R., Ramananarivo, S., Goyal, V., DeJong, J.T., Waller, J., Silk, W.K., 2015. The role of root development of Avena fatua in conferring soil strength. Am. J. Bot. 102, 1050–1060.

Eghrari, S., Ravanbakhsh, H., Shirvany, A., & Kartoolinejad, D., 2023. The effect of understory shrub species on the natural regeneration of Hyrcanian mixed broad-leaved forests (Kheyrud, Iran). Iranian Journal of Forest, 15(1), 1-10.

Eyvazi, M., 2014. The effect of forest roads on the introduction and establishment of invasive plant species (case study: Kheyrud forest, district Patom), MSc thesis, University of Tehran, 75 p (In Persian).

Fan, C.C., 2012. A displacement-based model for estimating the shear resistance of rootpermeated soils. Plant Soil, 355, 103–119.

Genet, M., Stokes, A., Salin, F., Mickovski, S.B., Fourcaud, T., Dumail, J.F., Vanbeek, R., 2005. The influence of cellulose content on tensile strength in tree roots. Plant Soil 258, 1–9.

Genet, M., Kokutse, N., Stokes, A., Fourcaud, T., Cai, X., Ji, J., Mickovski, S., 2008. Root reinforcement in plantations of Cryptomeria japonica D. Don: effect of tree age and stand structure on slope stability. Forest ecology and Management, 256(8), 1517-1526.

Giadrossich, F., Schwarz, M., Cohen, D., Cislaghi, A., Vergani, C., Hubble, T., Phillips, C. and Stokes, A., 2017. Methods to measure the mechanical behaviour of tree roots: A review. Ecological engineering, 109, pp.256-271.

Ghestem, M., Cao, K., Ma, W., Rowe, N., Leclerc, R., Gadenne, C., Stokes, A., 2014. A framework for identifying plant species to be used as 'ecological engineers' for fixing soil on unstable slopes. PLoS One 9, e95876.

Gholami-Derami, A., Akbari, H., Nasiri, M., Foshat, M., 2021. Comparison of bioengineering characteristics of native and non-native tree species. J. Wood For. Sci. Technol. 27, 67–80.

Gilardelli, F., Vergani, C., Gentili, R., Bonis, A., Chanteloup, P., Citterio, S., Chiaradia, E.A., 2017. Root Characteristics of Herbaceous Species for Topsoil Stabilization in Restoration Projects. Land Degrad. Dev. 28, 2074–2085.

Giupponi, L., Borgonovo, G., Giorgi, A., Bischetti, G.B., 2019. How to renew soil bioengineering for slope stabilization: some proposals. Landsc. Ecol. Eng. 15 (1), 37–50.

Gray, D.H., Sotir, R.B., 1996. *Biotechnical and soil bioengineering slope stabilization: a practical guide for erosion control*. John Wiley & Sons.

Hamidifar, H., Keshavarzi, A., Truong, P., 2018. Enhancement of river bank shear strength parameters using Vetiver grass root system. Arab. J. Geosci. 11, 611.

Hao, G., Liu, X., & Li, X. 2021. Quantification of additional cohesion from roots of mixed planting of multi-herb in dumping site and its influence on slope stability. Arabian Journal of Geosciences, 14, 1-15.

Hao, G., Wang, L., Liu, X., Zhang, Y., 2023. Geometric distribution characteristics and mechanical reinforcement effect of herbaceous plant roots at different growth periods. Soil Tillage Res. 229, 105682.

Hytiris, N., Fraser, M., Mickovski, S.B., 2015. Enhancing slope stability with vegetation. Int. J. Geomate 9, 1477–1482.

Inderjit, 2005. Plant invasions: habitat invasibility and dominance of invasive plant species. Plant and Soil, 277, 1-5.

Jennings, S.B., Brown, N.D., Sheil, D., 1999. Assessing forest canopies and understorey illumination: canopy closure, canopy cover and other measures. Forestry, 72(1), 59-74.

Karimi, Z., Abdi, E., Deljouei, A., Cislaghi, A., Shirvany, A., Schwarz, M., Hales, T.C. 2022. Vegetation-induced soil stabilization in coastal area: An example from a natural mangrove forest. Catena, 216, 106410.

Kettenhuber, P.L.W., dos Santos Sousa, R., Dewes, J.J., Rauch, H.P., Sutili, F.J., Hörbinger, S., 2023. Performance assessment of a soil and water bioengineering work on the basis of the flora development and its associated ecosystem processes. Ecol. Eng. 186, 106840.

Kim, J.H., Fourcaud, T., Jourdan, C., Maeght, J.L., Mao, Z., Metayer, J., Meylan, L., Pierret, A., Rapidel, B., Roupsard, O., de Rouw, A., Sanchez, M.V., Wang, Y., Stokes, A., 2017. Vegetation as a driver of temporal variations in slope stability: The impact of hydrological processes. Geophys. Res. Lett. 44, 4897–4907.

Kokutse, N.K., Temgoua, A.G.T., Kavazović, Z., 2016. Slope stability and vegetation: conceptual and numerical investigation of mechanical effects. Ecol. Eng. 86, 146–153.

Lann, T., Bao, H., Lan, H., Zheng, H., Yan, C., 2024. Hydro-mechanical effects of vegetation on slope stability: A review. Science of the Total Environment, 171691.

Liniger, H., Weingartner, R., 2000. Mountain forests and their role in providing freshwater resources. In *Forests in sustainable mountain development: a state of knowledge report for 2000. Task Force on Forests in Sustainable Mountain Development*. (pp. 370–380). Wallingford UK: CABI Publishing.

Loades, K.W., Bengough, A.G., Bransby, M.F., Hallett, P.D., 2010. Planting density influence on fibrous root reinforcement of soils. Ecol. Eng. 36, 276–284.

Löbmann, M.T., Geitner, C., Wellstein, C., Zerbe, S., 2020. The influence of herbaceous vegetation on slope stability – A review. Earth-Sci. Rev. 209, 103328.

Londo, G., 1976. The decimal scale for releves of permanent quadrats. Vegetation 33, 61–64.

Majnounian, B., Etter, H., 1992. Management plan for the district of Patom. Publication of Faculty of Natural Resources, University of Tehran. 102 pp.

Mao, Z., Roumet, C., Rossi, L.M., Merino-Martín, L., Nespoulous, J., Taugourdeau, O., Boukcim, H., Fourtier, S., Del Rey-Granado, M., Ramel, M., Ji, K., 2023. Intra-and interspecific variation in root mechanical traits for twelve herbaceous plants and their link with the root economics space. Oikos 1, p.e09032.

Mao, Z., Saint-André, L., Genet, M., Mine, F.X., Jourdan, C., Rey, H., Courbaud, B., Stokes, A., 2012. Engineering ecological protection against landslides in diverse mountain forests: Choosing cohesion models. Ecol. Eng. 45, 55–69.

Mao, Z., Wang, Y., McCormack, M.L., Rowe, N., Deng, X., Yang, X., Xia, S., Nespoulous, J., Sidle, R.C., Guo, D., Stokes, A., 2018. Mechanical traits of fine roots as a function of topology and anatomy. Ann. Bot. 122 (7), 1103–1116.

Masi, E.B., Segoni, S., Tofani, V., 2021. Root reinforcement in slope stability models: A review. Geosciences 11 (5), 212.

Masi, E.B.; Bicocchi, G.; Catani, F., 2020. Soil organic matter relationships with the geotechnical-hydrological parameters, mineralogy and vegetation cover of hillslope deposits in Tuscany (Italy). Bull. Eng. Geol. Environ. 79, 4005–4020.

Milledge, D.G., Bellugi, D., McKean, J.A., Densmore, A.L., Dietrich, W.E., 2014. A multidimensional stability model for predicting shallow landslide size and shape across landscapes: predicting landslide size and shape. J Geophys Res Earth Surf 119, 2481–2504.

Moghaddas, N.H., Ghafoori, M., 2007. Investigation of the distributions and causes of landslides in central Alborz, Iran. World Appl. Sci. J. 2, 652–657.

Mulyono, A., Subardja, A., Ekasari, I., Lailati, M., Sudirja, R., and Ningrum, W., 2018. The hydromechanics of vegetation for slope stabilization. In IOP Conference Series: Earth and Environmental Science (Vol. 118, p. 012038). IOP Publishing.

Murgia, I., Giadrossich, F., Mao, Z., Cohen, D., Capra, G.F. and Schwarz, M., 2022. Modeling shallow landslides and root reinforcement: A review. Ecol. Eng. 181, p.106671.

Pan, W.B., Bolton, R.P., Lundquist, E.J., Hiller, L.K., 1998. Portable rhizotron and color scanner system for monitoring root development. In *Root Demographics and Their Efficiencies in Sustainable Agriculture, Grasslands and Forest Ecosystems*; Box, J.E., Jr., Ed.; Springer: Dordrecht, Netherlands, pp. 745–756.

Pirasteh, S., Li, J., 2017. Landslides investigations from geoinformatics perspective: Quality, challenges, and recommendations. Geomatics, natural hazards and risk, 8(2), pp.448-465.

Pohl, M., Stroude, R., Buttler, A., Rixen, C., 2011. Functional traits and root morphology of alpine plants. Ann. Bot. 108, 537–545.

Pollen, N., Simon, A., 2005. Estimating the mechanical effects of riparian vegetation on stream bank stability using a fiber bundle model. Water Resources Research, 41(7), W07025. doi:10.1029/2004WR003801.

R Core Team, 2021. R: a language and environment for statistical computing. R Foundation for Statistical Computing, Vienna, Austria.

Rechinger, K.H., 1963. Flora Iranica. vols. 1-178. *Akademische Druck-U Verlagsanstalt, Graz*.

Rechinger, K.H., 1987. Flora Iranica, Vol. 162. *Akademische Druck-U Verlagsanstalt, Graz*.

Rey, F., Bifulco, C., Bischetti, G.B., Bourrier, F., De Cesare, G., Florineth, F., Graf, F., Marden, M., Mickovski, S.B., Phillips, C., Peklo, K., Poesen, J., Polster, D., Preti, F., Rauch, H.P., Raymond, P., Sangalli, P., Tardio, G., Stokes, A., 2019. Soil and water bioengineering: practice and research needs for reconciling natural hazard control and ecological restoration. Science of The Total Environment 648, 1210–1218. https://doi.org/10.1016/j.scitotenv.2018.08.217

Saadati, N., Mosaddeghi, M.R., Sabzalian, M.R., Jafari, M., 2023. Soil mechanical reinforcement by the fibrous roots of selected rangeland plants using a large soil-root shear apparatus. Soil Tillage Res. 234, 105852.

Sabeti, H. 1976. Forests, trees and shrubs of Iran. Ministry of Agriculture and natural Resources. 806 pp.

Saifuddin, M., Osman, N., Rahman, M.M., Boyce, A.N., 2015. Soil reinforcement capability of two legume species from plant morphological traits and mechanical properties. Curr. Sci., 1340–1347.

Sassa, K., Mikoš, M., Yin, Y., (Eds.). 2017. *Advancing Culture of Living with Landslides:* Volume 1 ISDR-ICL Sendai Partnerships 2015-2025. springer.

Schiechtl, H.M., 1980. *Bioengineering for Land Reclamation and Conservation*. (Edmonton: University of Alberta Press).

Schwarz, M., Giadrossich, F., Cohen, D., 2013. Modeling root reinforcement using a root-failure Weibull survival function. Hydrol. Earth Syst. Sci. 17 (11), 4367–4377.

Schwarz, M., Rist, A., Cohen, D., Giadrossich, F., Egorov, P., Buttner, D., Stolz, M., Thormann, J.J., 2015. Root reinforcement of soils under compression. J Geophys Res Earth Surf 120: 2103–2120.

Shakeri, Z., Marvie Mohadjer, M.R., Simberloff, D., Etemad, V., Assadi, M., Donath, T.W., Otte, A. and Eckstein, R.L., 2012. Plant community composition and disturbance in Caspian Fagus orientalis forests: which are the main driving factors. Phytocoenologia, 41(4), pp.247-263.

Shakeri, Z., Simberloff, D., Bernhardt-Römermann, M., Eckstein, R.L., 2021. The impact of livestock grazing and canopy gaps on species pool and functional diversity of ground flora in the Caspian beech forests of Iran. Appl Veg Sci. 24, e12592.

Siadati, S., Moradi, H., Attar, F., Etemad, V., Hamzeh'ee, B., Naqinezhad, A., 2010. Botanical diversity of Hyrcanian forests; a case study of a transect in the Kheyrud protected lowland mountain forests in northern Iran. Phytotaxa, 7(1), 1-18.

Smit, A.L., Bengough, A.G., Engels, C., van Noordwijk, M., Pellerin, S., van de Geijn, S.C., (Eds.). 2013. *Root methods: a handbook*. Springer Science & Business Media.

Stokes, A., Norris, J.E., van Beek, L.P.H., Bogaard, T., Cammeraat, E., Mickovski, S.B. (2008). Eco- and Ground Bio-Engineering: The Use of Vegetation to Improve Slope Stability. Springer, Dordrecht.

Stokes, A., Sotir, R.B., Chen, W., Ghestem, M., 2010. Soil bio- and eco-engineering in China, past experience and present priorities. Ecol. Eng. 36, 247–257.

Temgoua, A.G.T., Kokutse, N.K., Kavazović, Z., 2016. Influence of forest stands and root morphologies on hillslope stability. Ecol. Eng. 95, 622–634.

Terwilliger, V.J., Waldron, L.J., 1991. Effects of root reinforcement on soil-slip patterns in the Transverse Ranges of southern California. Geol. Soc. Am. Bull. 103 (6), 775–785.

Ujházyová, M., Ujházy, K., Máliš, F., Slezák, M., Hrivnák, R., 2021. Syntaxonomical revision of the order Fagetalia sylvaticae Pawłowski ex Pawłowski et al. 1928 in Slovakia. Biologia, 76(7), 1929-1968.

van der Maarel, E. 2005. Vegetation ecology–an overview. Vegetation Ecology, 3, 1-51.

931 Vergani, C., Schwarz, M., Cohen, D., Thormann, J.J., Bischetti, G.B., 2014. Effects of root
932 tensile force and diameter distribution variability on root reinforcement in the Swiss and
933 Italian Alps. Canadian Journal of Forest Research 44, 1426–1440.
934 https://doi.org/10.1139/cjfr-2014-0095

935 Vergani, C., Chiaradia, E.A., Bischetti, G.B., 2012. Variability in the tensile resistance of
936 roots in Alpine forest tree species. Ecol. Eng. 46, 43–56.

937 Vergani, C., Graf, F., 2015. Soil permeability, aggregate stability, and root growth: a pot
938 experiment from a soil bioengineering perspective. Ecohydrology 9, 830–842.

939 Waldron, L.J., 1977. The shear resistance of root-permeated homogeneous and stratified soil.
940 Soil Sci. Soc. Am. J. 41 (5), 843–849.

941 Wu, T.H., 1976. Investigation of landslides on Prince of Wales Island, Alaska. Ohio State
942 University, Department of Civil Engineering. Geotech Eng Rep 5:93

943 Wu, T.H., McKinnell III, W.P., Swanston, D.N., 1979. Strength of tree roots and landslides
944 on Prince of Wales Island, Alaska. Can. Geotech. J. 16 (1), 19–33.

945 Ye, C., Guo, Z., Li, Z., Cai, C., 2017. The effect of Bahiagrass roots on soil erosion
946 resistance of Aquults in subtropical China. Geomorphology 285, 82–93.

947 Zhang, C., Li, D., Jiang, J., Zhou, X., Niu, X., Wei, Y., Ma, J., 2019. Evaluating the potential
948 slope plants using new method for soil reinforcement program. Catena, 180, 346–354.

949 Zhong, R.H., He, X.B., Bao, Y.H., Tang, Q., Gao, J.Z., Yan, D.D., Wang, M.F., Li, Y., 2016.
950 Estimation of soil reinforcement by the roots of four post-dam prevailing grass species in the
951 riparian zone of three Gorges Reservoir, China. J. Mt. Sci. 13, 508–521.